Frequency-modulated comb LIDAR

Cite as: APL Photon. 4, 106105 (2019); doi: 10.1063/1.5120321
Submitted: 17 July 2019 • Accepted: 20 September 2019 •
Published Online: 9 October 2019

N. Kuse[1,a)] and M. E. Fermann[2]

AFFILIATIONS

[1]IMRA America, Inc., Boulder Research Labs, 1551 South Sunset St., Suite C, Longmont, Colorado 80501, USA
[2]IMRA America, Inc., 1044 Woodridge Ave., Ann Arbor, Michigan 48105, USA

[a)]**Current address:** Institute of Post-LED Photonics, Tokushima University, Tokushima, Japan. **Electronic mail:** kuse.naoya@tokushima-u.ac.jp.

ABSTRACT

Frequency-modulated continuous-wave LIDAR (FMCW LIDAR) has been widely used for both scientific and industrial tools. Here, in this report, a new class of LIDAR technique based on an optical frequency comb, named frequency-modulated comb LIDAR (FMcomb LIDAR), is proposed. Instead of using one carrier such as FMCW LIDAR, the multiple carriers from an optical frequency comb are used in FMcomb LIDAR. Because of the correlation between comb modes, each frequency-scanned comb mode can be coherently stitched, thus allowing for a resolution equivalent to scanning by many comb modes while scanning only by the comb mode spacing. In a proof-of-concept experiment, three comb modes from an electro-optic frequency comb (EO comb) are coherently stitched, showing Fourier-transform limited resolution (defined as FWHM linewidth) of 10 ps (i.e., 1.5 mm in air) for about 65 ns delay. The obtained resolution is three-times higher than that of conventional FMCW LIDAR when the same scan range is considered.

I. INTRODUCTION

LIDAR systems are ubiquitous in ranging, autonomous navigation, and surface profilometry.[1] One of the most powerful methods is based on the use of dual fiber frequency combs, enabling high resolution, high precision, and fast refresh rate.[2–4] However, the method requires two mutually phase locked frequency combs, making a system very complicated. To overcome this, dual electro-optic frequency combs (EO combs) have been used.[5,6] However, because of the large comb spacing of EO combs, the nonambiguous range (NAR) is very small, which is proportional to the inverse of the comb spacing. In addition, there are blind zones, where pulses from a reference and target plains in an interferometer are overlapped and the targets cannot be distinguished. This is why frequency-modulated continuous-wave (FMCW) LIDAR[7–9] remains to be popular in the real world. In FMCW LIDAR, since the NAR can be extremely large, an actual limit for the measurable range is set by the coherence length of the used cw laser, which is proportional to the inverse of the cw laser linewidth. The achievable resolution is proportional to the inverse of the scanning frequency range of the cw laser. These two constraints make a trade-off between the measurable range and resolution. For example, micro-electro-mechanically tuned vertical-cavity surface-emitting lasers (MEMS-VCSELs) with 100 nm scan range with 100 kHz sweep rate are commercially available (e.g., Thorlabs, Inc., SL131090), but their coherence length is as short as a few meters, which corresponds to linewidth of about 100 MHz. On the other hand, metrology-grade external cavity lasers (ECLs) have very narrow linewidth (~1 kHz), but the fast scanning range is only 200 MHz (e.g., RIO ORION Laser Module). The trade-off is a fundamental issue because longer cavities are required for narrow linewidth, but longer cavities do not allow fast, large scanning range without mode-hopping because of the smaller free spectral range (FSR) of the laser.

To overcome the trade-off, coherent stitching of multiple distributed-feedback lasers (DFB lasers) has been demonstrated.[10,11] The DFB lasers have moderately narrow linewidth (~1 MHz) and allow fast scanning for a scan range of about 1 nm. By coherently stitching more than 100 DFB lasers with a scan range of 1 nm, a large measurable range (>100 m) with high resolution (<10 μm) can be, in principle, obtained. However, the more the DFB lasers are required, the more complicated the system becomes. In addition, since both the knowledge of the chirp rate (=scan range/scan time) and the instantaneous frequency (from an offset frequency)

are required for coherent stitching of uncorrelated cw lasers, perfect coherent stitching is difficult when several cw lasers or long distance measurements are considered. For example, in Ref. 11, an external reference based on molecular absorption is used to extract the chirp rate and instantaneous frequency, which potentially causes imperfect coherent stitching because of the limited number of absorption lines and absorption linewidth. Whilst the above methods are based on wavelength division multiplexing (WDM), alternatively, several comb modes from a mode-locked laser can also be combined via time division multiplexing (TDM).[12,13] However, with TDM, the scan time increases with the number of channels, whereas in WDM, all channels are detected simultaneously. TDM also faces additional challenges such as the requirement of an EO modulator and careful delay adjustment for each channel.

In this letter, we propose frequency-modulated comb LIDAR (FMcomb LIDAR), in which the comb modes of a frequency comb, generated from a single cw laser (rather than from multiple, independent cw lasers), are coherently stitched. Because of the correlated relationship between the comb modes, chirp rate and instantaneous frequency of the comb modes can be known in a precise and simple manner. In the proposed idea, a single reference interferometer with known delay is sufficient for coherent stitching and to correct for deviations from linear scanning. In a proof-of-concept demonstration, three comb modes from an EO comb are coherently stitched, resulting in three times higher Fourier-transform limited resolution (10 ps, i.e., 1.5 mm in the air, defined as FWHM linewidth) than that of the conventional FMCW LIDAR for about 65 ns delay.

II. WORKING PRINCIPLE

The setup to realize the proposed idea and working principle is shown in Fig. 1. A frequency-scanned cw laser (center frequency of ν_0) is split along two paths. One path contains a reference interferometer, whose purposes are described later. The other is used to generate a frequency comb [either EO comb[14,15] or comb generated from a microresonator (microcomb)[16,17]] with a comb spacing of Δ, which is measured constantly. The generated frequency comb is directed to a target interferometer, followed by a wavelength division multiplexer (WDM) to separate each comb mode. For simplicity, we assume an ideal WDM, as shown in Fig. 1(b), in which the Kth channel transmits light with an optical frequency between $\nu_0 + (K-1)\Delta$ and $\nu_0 + K\Delta$. The separated comb modes are photo-detected and digitized for signal processing. Figure 1(c) (left) shows the instantaneous frequencies of the comb modes with frequency scanning. Here, we assume that the comb spacing of the frequency comb is fixed and the carrier envelope offset frequency is scanned, which is true for EO combs, and the frequency scan is purely linear. The supplementary material shows a general case, in which both the comb spacing and the carrier envelope offset frequency are involved in scanning. All the comb modes are scanned a little more than the comb spacing, producing an overlapping instantaneous frequency between the (K − 1)th and (K − 2)th comb modes in the Kth channel. If the cycle time (expressed as T_{cycle}) which is the time it takes for the cw laser to be scanned by the comb spacing is known, all comb modes can be coherently stitched, as shown in Fig. 1(c) (right), which is more explicitly shown in Fig. 1(d). Figure 1(d) shows the

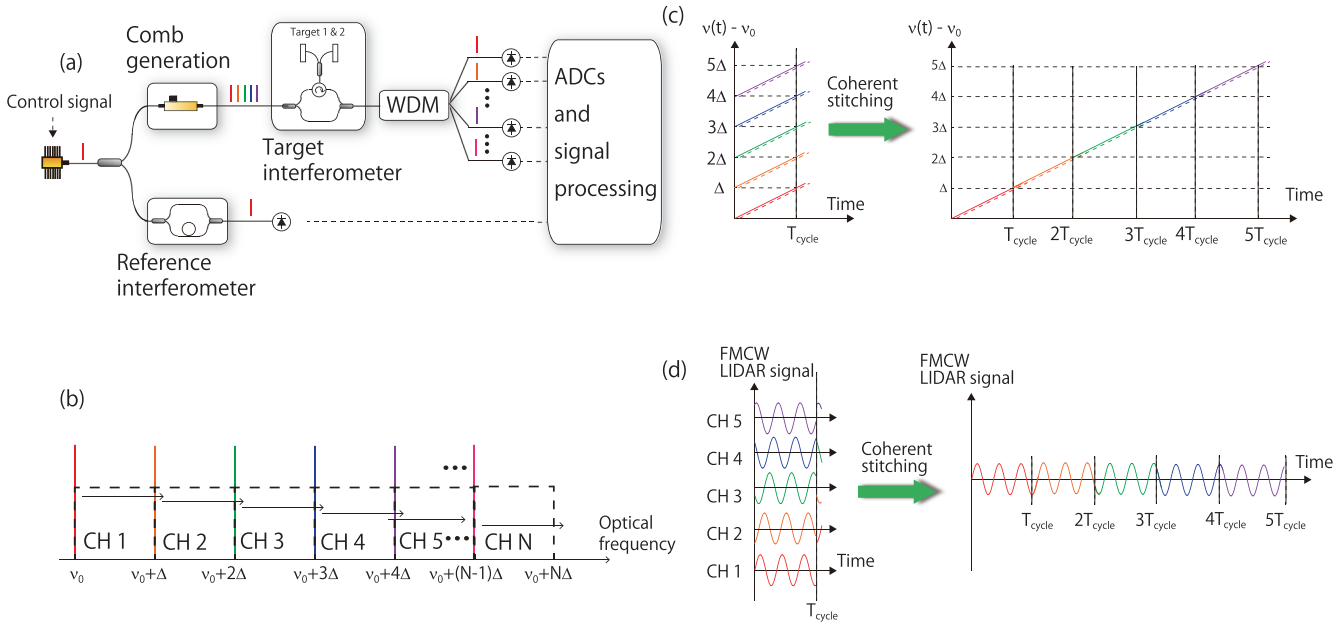

FIG. 1. Concept of FMcomb LIDAR. (a) Schematic of the FMcomb LIDAR system. Colors stand for the wavelength of the comb modes. (b) Allocation of the channels by WDM. The dashed squares show the transmission of the channels. Here, for simplicity, the transmission function is assumed to have a perfect square shape. (c) Working principle with instantaneous frequencies. Solid and dashed lines show the comb modes without and with the delay in the target interferometer, respectively. (d) Working principle with FMCW LIDAR signals, which are generated from photodetectors. The signals jump at T_{cycle} because the photo-detected comb mode is switched from the Kth to (K − 1)th comb mode, satisfying $\varphi_K(t) = \varphi_K(t + T_{\mathrm{cycle}})$ $(0 \le t < \varepsilon)$.

working principle explained by the use of FMCW LIDAR signals. The Kth channel sees the same signal at time = 0 + t and time = T_{cycle} + t ($0 \le t < \varepsilon$), where ε is a small positive quantity, because the instantaneous frequency becomes the same at these times. An FMCW LIDAR signal with an effective length of $N \times T_{cycle}$ can be obtained by coherently stitching the FMCW LIDAR signals, where the 1st channel produces the signal for time 0–T_{cycle}, the 2nd channel for T_{cycle}–$2T_{cycle}$…, and the Nth channel for $(N-1)T_{cycle}$–NT_{cycle}. By coherent stitching of the frequency comb with N comb modes, an N time larger range scan can be obtained, enhancing the resolution of the LIDAR system by N times, realizing both high resolution and large coherence length because the need for a large scan range is obviated.

A key to the proposed idea is that the Kth channel sees the same signal at time = 0 + t and time = T_{cycle} + t ($0 \le t < \varepsilon$), which is mathematically verified as below. The electric field of the Kth frequency comb mode from the cw laser with a linear frequency scan [$E_K(t)$] can be expressed as

$$E_K(t) = e^{2\pi i\left\{(\nu_0+K\Delta)t+\frac{\Delta}{2T_{cycle}}t^2\right\}}. \quad (1)$$

The electric field for the (K + 1)th channel just before a photodetector ($0 \le t < T_{cycle}$) is $E_K(t) + E_K(t-\tau)$ and generates a photo-detected signal [$V_K(t)$] as

$$V_K(t) = |E_K(t) + E_K(t-\tau)|^2 \propto \cos 2\pi\left\{\frac{\Delta}{T_{cycle}}\tau t + (\nu_0 + K\Delta)\tau - \frac{\Delta}{2T_{cycle}}\tau^2\right\}. \quad (2)$$

Here, the DC term is ignored. In ($T_{cycle} \le t < T_{cycle} + \varepsilon$), instead of the Kth comb mode, the (K − 1)th EO comb mode enters in the (K + 1) th channel, generating a FMCW LIDAR signal as

$$V_K(t) = |E_{K-1}(t) + E_{K-1}(t-\tau)|^2 \propto \cos 2\pi\left\{\frac{\Delta}{T_{cycle}}\tau t + (\nu_0 + (K-1)\Delta)\tau - \frac{\Delta}{2T_{cycle}}\tau^2\right\}. \quad (3)$$

Looking at the phase [$\varphi_K(t)$] of $V_K(t)$, $\varphi_K(t) = \varphi_K(t + T_{cycle})$ ($0 \le t < \varepsilon$) is satisfied, which means that the FMCW LIDAR signals between the channels can be coherently stitched. In addition, having frequency overlap for ($0 \le t < \varepsilon$ and $T_{cycle} \le t < T_{cycle} + \varepsilon$) is advantageous for amplitude correction and reducing the required accuracy for the reference interferometer. Via signal processing, $\varphi_K(t) = \varphi_K(t + T_{cycle})$ can be enforced to ensure perfect coherent stitching as long as the phase mismatch is guaranteed to be within $\pm\pi$. In this case, ultimate accuracy is determined by the reference for the comb spacing (i.e., Rb clock in this experiment).

For coherent stitching, T_{cycle} should be known in advance. A reference interferometer, which consists of an imbalanced Mach-Zehnder interferometer (MZI), is used for this, whose delay between the two arms (τ_{ref}) is accurately known. With the known delay, T_{cycle} can be obtained as

$$T_{cycle} = \frac{\Delta}{f_{beat,\,ref}} \cdot \tau_{ref}. \quad (4)$$

Here, $f_{beat,ref}$ is the frequency of the FMCW LIDAR signal for the reference interferometer. With moderate temperature stabilization, a reference interferometer made by a fiber interferometer with 6 digit accuracy (10^{-6}) of the delay (τ_{ref}) can be obtained because the thermal expansion coefficient of silica fiber, including both thermal and thermo-optic effects, is about 10^{-5}/K.[18,19] Assuming 6 digit accuracy of the delay and a 100 GHz comb spacing with the allowable $\pm\pi$ phase mismatch, more than 10 μs delay in a target interferometer ($\tau_{target} < \frac{\text{allowable phase mismatch}}{2\pi \times \text{accuracy} \times \Delta}$) can be measured.

III. EXPERIMENT

An experimental setup is shown in Fig. 2(a). A cw laser (Toptica, CTL1550) based on an external cavity diode laser with about 1550 nm center wavelength and <10 kHz linewidth is used, which is modulated with a chirp rate of about 1 THz/s. Note that cw lasers

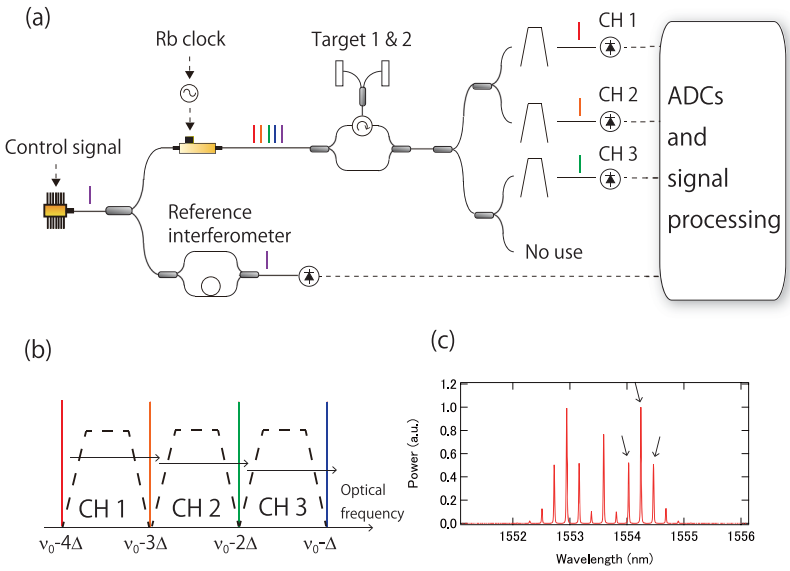

FIG. 2. (a) Schematic of the experimental setup. (b) Allocation of the channels by the BPFs. (c) Optical spectrum of the EO comb. The arrows show the used comb modes in the experiment.

based on DFB lasers with broader linewidth and larger chirp rate fully utilize the proposed idea, enabling a low cost LIDAR system with a high resolution and fast scan rate in addition to a large measurable range. An EO comb with a comb spacing of 26.9867 GHz (Anritsu, MG3693B), which is referenced to an Rb clock, is generated by phase-modulating the cw laser [Fig. 2(c)]. The EO comb is directed to a target interferometer, which consists of a fiber MZI. One arm of the MZI can have two paths to emulate a case with two targets. The delay between the two arms is about 65 ns, which corresponds to about 13 m fiber length difference, including single and double fiber path. A WDM is made by optical fiber splitters and optical bandpass filters. Because of limited equipment in our lab, three comb modes (-2nd, -3rd, and -4th modes of the EO comb) are used in this experiment. Channels are allocated as shown in Fig. 2(b). The center of the passband of the optical bandpass filters is set at about the middle of the channels (e.g., $\nu_0 - 3.5\Delta$ for CH 1). The bandwidth of the optical bandpass filters is set as large as possible, while making sure that the simultaneous detection of two next neighbor comb modes is prevented. The filtered light is photo-detected, digitized (RIGOL, DS1054Z), and signal-processed offline. Part of the cw laser also goes through a reference interferometer. The reference interferometer consists of a fiber MZI with 36.9441 ns delay, which is measured by a separate experiment with about 5 digit accuracy. The FMCW LIDAR signal from the reference interferometer is used for nonlinear scanning correction and to verify T_{cycle}. The nonlinearity is caused by the nonlinear response of the cw laser to a linear control signal.

Figures 3(a)–3(c) show FMCW LIDAR signals for CH 1, 2, and 3 after signal processing. The signal processing includes DC removal, nonlinear scanning correction,[20–23] amplitude correction from the transmission loss difference between channels, and amplitude correction from the power difference between comb modes. Nonlinear scanning correction is realized by picking up zero crossings of the FMCW LIDAR signal for the reference channel. Then, new time axis is made by interpolating sampling points between the zero crossings (more details are shown in the supplementary material). The FMCW LIDAR signals for CH 1 come from the -4th EO comb mode for $0 \le t <$ ~25 ms and the -5th EO comb mode for $t >$ ~25 ms (we do not use the data). In the same way, the FMCW LIDAR signal for the CH 2 sees the -3rd and the -4th EO comb modes, and that for the CH 4 sees the -2nd EO comb mode and the -3rd EO comb mode. Note that negligibly small optical signals hit the photodetectors around 25 ms to clearly know which comb modes are detected.

As explained in Sec. II, the FMCW LIDAR signals should satisfy $\varphi_{\mathrm{K}}(t) = \varphi_{\mathrm{K}}(t + T_{\mathrm{cycle}})$. Figures 3(d) and 3(e) show the magnified FMCW LIDAR signals for CH 2 with a separation time of T_{cycle} estimated from the reference interferometer. Even without any timing correction, the phase mismatch is within 30 mrad. Note that we did not implement timing correction for all experimental data shown in this paper.

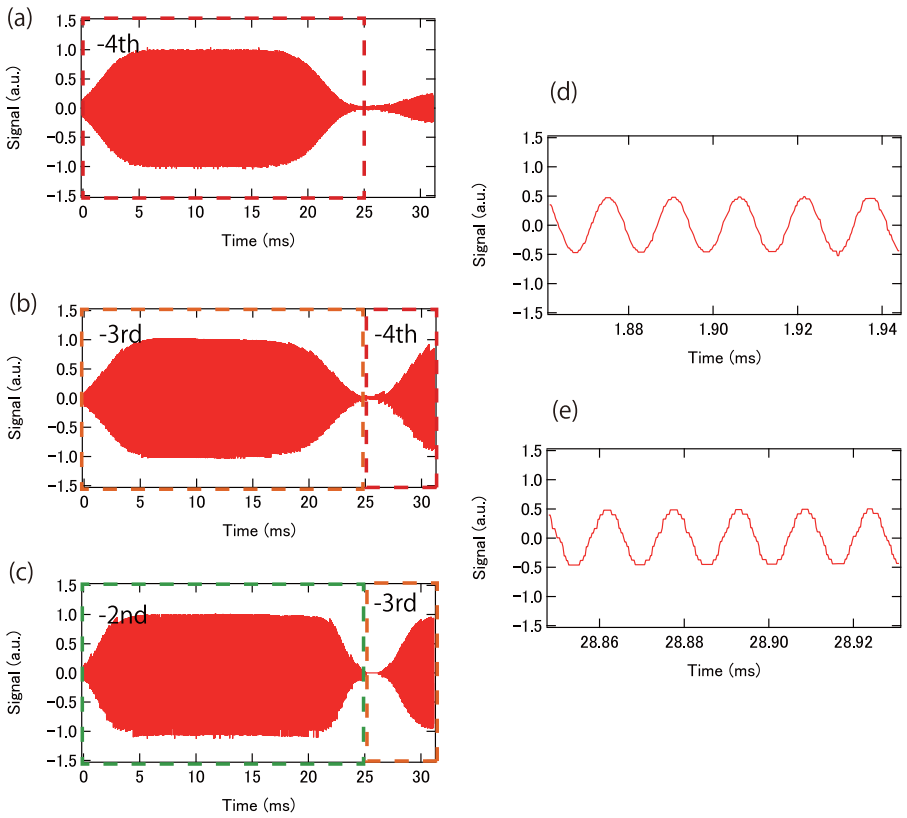

FIG. 3. [(a)–(c)] FMCW LIDAR signals for CH1, 2, and 3. The dashed squares show which comb modes are detected at the channels. [(d) and (e)] Magnified FMCW LIDAR signals for CH2 separated by T_{cycle} estimated from the reference interferometer.

Figure 4(a) shows a coherently stitched FMCW signal, which shows an effective scan range of 3Δ. A Fourier transform of the stitched FMCW LIDAR signal is shown in Fig. 4(b) (red curve). Compared with a conventional FMCW LIDAR with a scan range of Δ, three times higher resolution is obtained (10 ps for FMcomb LIDAR and 30 ps for FMCW LIDAR). In addition, the Fourier transform of an ideal FMcomb LIDAR, which consists of a pure sine function with a given filter shape as used in the experiment is also shown in Fig. 4(b) (black dashed curve). The FMcomb LIDAR shows different sidebands from the conventional FMCW LIDAR, which originates from amplitude modulation from the optical bandpass filters. Although the optical bandpass filters cannot be as ideal as shown in Fig. 2(b), use of an optical frequency comb with a larger comb spacing such as provided by microcombs generates a Fourier transformed signal which is more similar to conventional FMCW LIDAR, ignoring the amplitude modulation effect from the optical bandpass filters.

Finally, two-target detection is also demonstrated. As shown in Fig. 2(a), instead of using two closely located targets, we use two targets with similar delays for experimental convenience. In the results, FMcomb LIDAR is compared with conventional FMCW LIDAR with a scan range of Δ. As shown in Fig. 5(a), when the two targets are moderately separated, both FMcomb LIDAR and FMCW LIDAR resolve the two targets. However, when the two targets are closer [Fig. 5(b)], FMCW LIDAR cannot distinguish the two targets, showing a single peak with an asymmetric shape. On the other hand, FMcomb LIDAR clearly distinguishes the two targets, showing two peaks. The subpeaks in Fig. 5(b) are superpositions of the sidebands from each target.

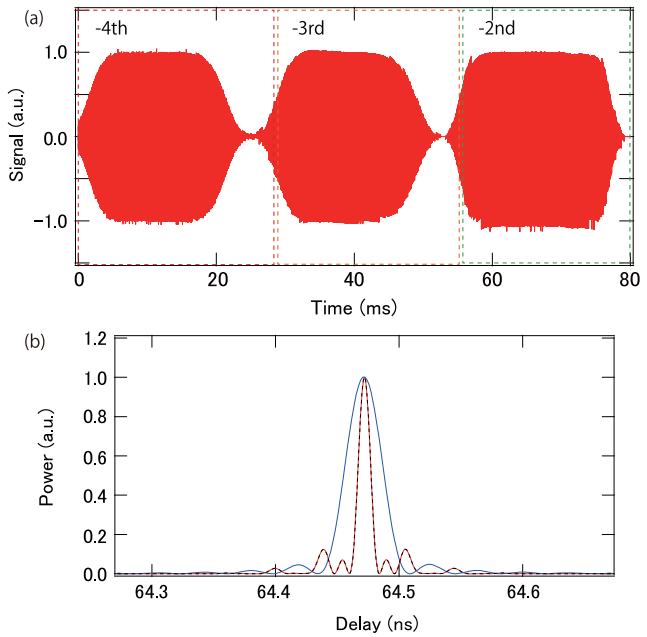

FIG. 4. (a) Coherently stitched FMCW LIDAR signal, i.e., FMcomb LIDAR signal. Dashed lines show which comb modes are used. (b) (Red) Estimated delay from (a). (Blue) Estimated from the conventional FMCW LIDAR with the same scan range. (Black dashed) Fourier transform of an ideal FMcomb LIDAR.

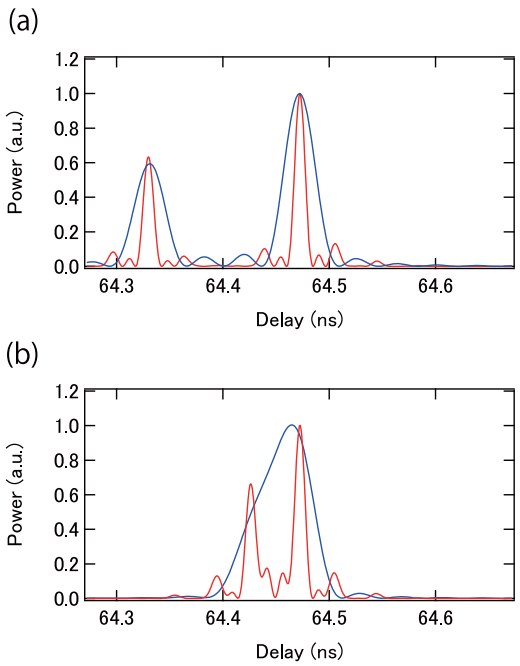

FIG. 5. FMcomb LIDAR with two targets. Estimated delay with moderately separated targets (a) and a closely located targets (b). (Blue) Estimated delay from the conventional FMCW LIDAR with the same scan range.

IV. DISCUSSION AND CONCLUSION

In the experiment, a quite bulky and expensive cw laser (Toptica, CTL 1550) based on an ECL is used, which has good instantaneous linewidth (<10 kHz) and scans relatively slowly (1 THz/s in the experiment). However, an optical frequency comb can be also generated from a DFB laser, which has larger linewidth (~1 MHz) and fast scanning (1 PHz/s), to fully utilize the proposed idea, i.e., to overcome the trade-off between the high resolution and large measurable range (or fast measurement). When many comb modes are used, it may be better to have similar intensities for the comb modes, even if signal processing can compensate intensity variations. There are reports about generating EO combs with flat optical spectra.[24,25] Although, with an increasing number of comb modes, the resolution increases, there is a trade-off between the measurable distance and range resolution. In general, the measurable distance decreases with the number of comb modes N as $\sqrt{N}$ compared to FMCW LIDAR with the same setup and the same average optical power. Although one may also worry about the phase noise degradation of the EO comb with harmonic mode numbers,[15,26] the phase noise magnification can be ignored, especially when cw lasers with >10 kHz linewidth are used. For the future integration of the FMcomb LIDAR system to minimize size and cost, arrayed waveguide gratings (AWGs),[27,28] which are matured in silicon photonics, can be used instead of bulky optical BPFs used in the proof-of-concept demonstration. Photodetectors (PDs) can also be integrated in the same platform as AWGs. Furthermore, following rapid progress of microcombs,[29–31] FMcomb LIDAR based on microcombs will provide highly integrated, potentially low cost solutions with greatly

improved size, weight, and power (SWaP) requirements. However, when a microcomb is used, one additional signal processing to compensate the comb spacing change is required, as explained in the supplementary material. Note that we have already demonstrated a proof-of-concept experiment of a continuous scanning of a dissipative Kerr-microresonator soliton comb.[32]

In conclusion, we proposed a new type of LIDAR based on an optical frequency comb, named FMcomb LIDAR, which overcomes a trade-off between the resolution and measurable range in conventional FMCW LIDAR. In FMcomb LIDAR, the frequency-modulated comb modes of an optical frequency comb are coherently stitched, enabling an effectively larger scan range proportional to the number of stitched comb modes. In the proof-of-concept experiment, FMcomb LIDAR has been demonstrated by using the three comb modes from an EO comb. As expected, three times higher resolution was obtained, compared with the conventional FMCW LIDAR. In conjunction with microcombs and chip-scale AWGs and PDs, FMcomb LIDAR can be a low cost, potentially chip scale LIDAR system with a high resolution (<15 μm, which is equivalent to 100 comb modes for a 100 GHz comb spacing) and large measurable range (>100 m), making it simultaneously useable for both long-distance and precision ranging applications.

SUPPLEMENTARY MATERIAL

See supplementary material for a mathematical expression for signal processing when both carrier envelope offset frequency and comb spacing are scanned, targeting use of microcombs. In addition, the method implemented for nonlinear scanning correction is described.

ACKNOWLEDGMENTS

We acknowledge Tomohiro Tetsumoto for fruitful discussions.

REFERENCES

[1]M.-C. Amann, T. M. Bosch, M. Lescure, R. A. Myllylae, and M. Rioux, "Laser ranging: A critical review of unusual techniques for distance measurement," Opt. Eng. **40**, 10–20 (2001).
[2]I. Coddington, W. C. Swann, L. Nenadovic, and N. R. Newbury, "Rapid and precise absolute distance measurements at long range," Nat. Photonics **3**, 351 (2009).
[3]J. Lee, S. Han, K. Lee, E. Bae, S. Kim, S. Lee, S.-W. Kim, and Y.-J. Kim, "Absolute distance measurement by dual-comb interferometry with adjustable synthetic wavelength," Meas. Sci. Technol. **24**, 045201 (2013).
[4]H. Zhang, H. Wei, X. Wu, H. Yang, and Y. Li, "Absolute distance measurement by dual-comb nonlinear asynchronous optical sampling," Opt. Express **22**, 6597–6604 (2014).
[5]R. Yang, F. Pollinger, K. Meiners-Hagen, J. Tan, and H. Bosse, "Heterodyne multi-wavelength absolute interferometry based on a cavity-enhanced electro-optic frequency comb pair," Opt. Lett. **39**, 5834–5837 (2014).
[6]X. Zhao, X. Qu, F. Zhang, Y. Zhao, and G. Tang, "Absolute distance measurement by multi-heterodyne interferometry using an electro-optic triple comb," Opt. Lett. **43**, 807–810 (2018).
[7]D. Uttam and B. Culshaw, "Precision time domain reflectometry in optical fiber systems using a frequency modulated continuous wave ranging technique," J. Lightwave Technol. **3**, 971–977 (1985).
[8]E. Baumann, F. R. Giorgetta, I. Coddington, L. C. Sinclair, K. Knabe, W. C. Swann, and N. R. Newbury, "Comb-calibrated frequency-modulated continuous-wave ladar for absolute distance measurements," Opt. Lett. **38**, 2026–2028 (2013).
[9]C. V. Poulton, A. Yaacobi, D. B. Cole, M. J. Byrd, M. Raval, D. Vermeulen, and M. R. Watts, "Coherent solid-state LIDAR with silicon photonic optical phased arrays," Opt. Lett. **42**, 4091–4094 (2017).
[10]A. Vasilyev, N. Satyan, S. Xu, G. Rakuljic, and A. Yariv, "Multiple source frequency-modulated continuous-wave optical reflectometry: Theory and experiment," Appl. Opt. **49**, 1932–1937 (2010).
[11]T. DiLazaro and G. Nehmetallah, "Multi-terahertz frequency sweeps for high-resolution, frequency-modulated continuous wave ladar using a distributed feedback laser array," Opt. Express **25**, 2327–2340 (2017).
[12]K. W. Holman, D. G. Kocher, and S. Kaushik, "MIT/LL development of broadband linear frequency chirp for high-resolution ladar," Proc. SPIE **6572**, 65720J (2007).
[13]K. W. Holman, "200-GHz 8-μs LFM optical waveform generation for high-resolution coherent imaging," in *19th Coherent Laser Radar Conference* (2018), p. Th7.
[14]D. R. Carlson, D. D. Hickstein, W. Zhang, A. J. Metcalf, F. Quinlan, S. A. Diddams, and S. B. Papp, "Ultrafast electro-optic light with subcycle control," Science **361**, 1358–1363 (2018).
[15]A. Ishizawa, T. Nishikawa, A. Mizutori, H. Takara, A. Takada, T. Sogawa, and M. Koga, "Phase-noise characteristics of a 25-GHz-spaced optical frequency comb based on a phase-and intensity-modulated laser," Opt. Express **21**, 29186–29194 (2013).
[16]P. Del'Haye, A. Schliesser, O. Arcizet, T. Wilken, R. Holzwarth, and T. J. Kippenberg, "Optical frequency comb generation from a monolithic microresonator," Nature **450**, 1214 (2007).
[17]T. Herr, V. Brasch, J. D. Jost, C. Y. Wang, N. M. Kondratiev, M. L. Gorodetsky, and T. J. Kippenberg, "Temporal solitons in optical microresonators," Nat. Photonics **8**, 145 (2014).
[18]R. Slavík, G. Marra, E. N. Fokoua, N. Baddela, N. V. Wheeler, M. Petrovich, F. Poletti, and D. J. Richardson, "Ultralow thermal sensitivity of phase and propagation delay in hollow core optical fibres," Sci. Rep. **5**, 15447 (2015).
[19]E. N. Fokoua, M. N. Petrovich, T. Bradley, F. Poletti, D. J. Richardson, and R. Slavík, "How to make the propagation time through an optical fiber fully insensitive to temperature variations," Optica **4**, 659–668 (2017).
[20]T.-J. Ahn, J. Y. Lee, and D. Y. Kim, "Suppression of nonlinear frequency sweep in an optical frequency-domain reflectometer by use of Hilbert transformation," Appl. Opt. **44**, 7630–7634 (2005).
[21]P. A. Roos, R. R. Reibel, T. Berg, B. Kaylor, Z. W. Barber, and W. R. Babbitt, "Ultrabroadband optical chirp linearization for precision metrology applications," Opt. Lett. **34**, 3692–3694 (2009).
[22]T. Zhang, X. Qu, and F. Zhang, "Nonlinear error correction for FMCW ladar by the amplitude modulation method," Opt. Express **26**, 11519–11528 (2018).
[23]P. Feneyrou, L. Leviandier, J. Minet, G. Pillet, A. Martin, D. Dolfi, J.-P. Schlotterbeck, P. Rondeau, X. Lacondemine, A. Rieu *et al.*, "Frequency-modulated multifunction lidar for anemometry, range finding, and velocimetry—2. Experimental results," Appl. Opt. **56**, 9676–9685 (2017).
[24]T. Sakamoto, T. Kawanishi, and M. Izutsu, "Asymptotic formalism for ultraflat optical frequency comb generation using a Mach-Zehnder modulator," Opt. Lett. **32**, 1515–1517 (2007).
[25]Q. Wang, L. Huo, Y. Xing, and B. Zhou, "Ultra-flat optical frequency comb generator using a single-driven dual-parallel Mach-Zehnder modulator," Opt. Lett. **39**, 3050–3053 (2014).
[26]N. Kuse, T. R. Schibli, and M. E. Fermann, "Low noise electro-optic comb generation by fully stabilizing to a mode-locked fiber comb," Opt. Express **24**, 16884–16893 (2016).
[27]M. K. Smit and C. Van Dam, "PHASAR-based WDM-devices: Principles, design and applications," IEEE J. Sel. Top. Quantum Electron. **2**, 236–250 (1996).
[28]C. Doerr, L. Stulz, and R. Pafchek, "Compact and low-loss integrated box-like passband multiplexer," IEEE Photonics Technol. Lett. **15**, 918–920 (2003).
[29]B. Stern, X. Ji, Y. Okawachi, A. L. Gaeta, and M. Lipson, "Battery-operated integrated frequency comb generator," Nature **562**, 401 (2018).

[30]A. S. Raja, A. S. Voloshin, H. Guo, S. E. Agafonova, J. Liu, A. S. Gorodnitskiy, M. Karpov, N. G. Pavlov, E. Lucas, R. R. Galiev *et al.*, "Electrically pumped photonic integrated soliton microcomb," Nat. Commun. **10**, 680 (2019).
[31]S. Zhang, J. M. Silver, L. Del Bino, F. Copie, M. T. Woodley, G. N. Ghalanos, A. Ø. Svela, N. Moroney, and P. Del'Haye, "Sub-milliwatt-level microresonator solitons with extended access range using an auxiliary laser," Optica **6**, 206–212 (2019).
[32]N. Kuse, T. Tetsumoto, Y. Xuan, and M. Fermann, "Continuous scanning of a dissipative Kerr-microresonator soliton comb by Pound-Drever-Hall locking," in *CLEO: Science and Innovations* (Optical Society of America, 2019), p. SF2I–5.